

ORIGINAL ARTICLE

Urinary metabolomics (GC-MS) reveals that low and high birth weight infants share elevated inositol concentrations at birth

Luigi Barberini¹, Antonio Noto², Claudia Fattuoni³, Dmitry Grapov⁴, Andrea Casanova⁵, Gianni Fenu⁶, Mauro Gaviano⁶, Roberta Carboni², Giovanni Ottonello², Maurizio Crisafulli², Vassilios Fanos², and Angelica Dessì²

¹Department of Public Health Clinical and Molecular Medicine, University of Cagliari, Cagliari, Italy, ²Department of Surgical Sciences, Neonatal Intensive Care Unit, Puericulture Institute and Neonatal Section, Azienda Ospedaliera Universitaria, Cagliari, Italy, ³Department of Chemical and Geological Sciences, University of Cagliari, Cagliari, Italy, ⁴NIH West Coast Metabolomics Center, University of California Davis, Davis, CA, USA, ⁵Department of Medical Sciences "M. Aresu", University of Cagliari, Cagliari, Italy, and ⁶Department of Mathematics and Informatics, University of Cagliari, Cagliari, Italy

Abstract

Objective: Metabolomics is a new "omics" platform aimed at high-throughput identification, quantification and characterization of small molecule metabolites. The metabolomics approach has been successfully applied to the classification different physiological states and identification of perturbed biochemical pathways. The purpose of the current investigation is the application of metabolomics to explore biological mechanisms which may lead to the onset of metabolic syndrome in adulthood.

Methods: We evaluated differences in metabolites in the urine collected within 12 hours from 23 infants with IUGR (IntraUterine Growth Restriction), or LGA (Large for Gestational Age), compared to control infants (10 patients defined AGA: Appropriate for Gestational Age). Urinary metabolites were quantified by GC-MS and used to highlight similarities between the two metabolic diseases and identify metabolic markers for their predisposition. Quantified metabolites were analyzed using a multivariate statistics coupled with receiver operator characteristic curve (ROC) analysis of identified biomarkers.

Results: Urinary myo-inositol was the most important discriminant between LGA + IUGR and control infants, and displayed an area under the ROC curve = 1.

Conclusion: We postulate that the increase in plasma and consequently urinary inositol may constitute a marker of altered glucose metabolism during fetal development in both IUGR and LGA newborns.

Introduction

Progress in new systems biology methodologies which study metabolic alterations of aetiological processes at the origin of many pathologies are becoming more important. In particular, metabolomics, a new analytical technique defined as the study of the complex system of metabolites, is capable of describing the biochemical phenotype of a biological system [1]. At present, attention is being focused mainly on the formulation of new hypotheses concerning the biological mechanisms that lead to the onset of diabetes and metabolic syndrome in adulthood. Metabolomics has been recently applied to identify several biomarkers (including myo-inositol) for mechanisms which may lead to infantile obesity and the subsequent onset of metabolic diseases [2].

Comprehensive analysis of changes in metabolic profiles during fetal and neonatal life may present an important reference for understanding fundamental biochemical mechanisms, which may lead to consequent metabolic alterations. Previous investigations have demonstrated that fetal malnutrition, whether excessive (overnutrition) or insufficient (hyponutrition), can permanently alter the fetus's metabolic state and increase the risk of chronic diseases later in life. This suggests that neonates with intrauterine growth retardation (IUGR) and large-for-gestational-age (LGA) neonates, despite opposing metabolic characteristics during fetal life, at birth may exhibit a common condition of reduced glucose tolerance which can persist into adulthood, and consequently leads to an increased risk of developing metabolic syndrome related pathologies such as obesity and type 2 diabetes [3]. The current investigation compared urine metabolic profiles of IUGR and LGA neonates to controls to identify metabolic similarities between IUGR and LGA and to identify markers for biochemical alterations during fetal life which may lead to the onset of metabolic syndrome in adulthood.

Address for correspondence: Prof. Vassilios Fanos, Director Neonatal Intensive Care Unit, Puericulture Institute and Neonatal Section, University of Cagliari, Cagliari 09124, Italy. Tel: +3907051093403 (direct); +3907051093438 (NICU). E-mail: vafanos@tin.it; vafanos@tiscali.it

Keywords

GC-MS, inositol, IUGR, metabolomics, OSC-PLS-DA

History

Received █
 Revised █
 Accepted █
 Published online █ █ █

61
62
63
64
65
66
67
68
69
70
71
72
73
74
75
76
77
78
79
80
81
82
83
84
85
86
87
88
89
90
91
92
93
94
95
96
97
98
99
100
101
102
103
104
105
106
107
108
109
110
111
112
113
114
115
116
117
118
119
120

121 Methods

122 Patient cohort and sample collection

123 This study was carried out on urine samples of three groups of
 124 patients admitted to the Neonatal Intensive Care Unit (NICU)
 125 and Puericulture of the University of Cagliari. Ethical
 126 committee approved the study protocol and written informed
 127 consent was obtained from the parents before enrolment in the
 128 study. The first group included 11 IUGR patients (5 males and
 129 6 females) diagnosed with ultrasonography in the prenatal
 130 period [4] and with birth weight below the 10th percentile
 131 (mean gestational age 37.1). The second group comprised 12
 132 LGA neonates (7 males and 5 females) with birth weight
 133 above the 90th percentile (mean gestational age 37.6) while
 134 the third group included 10 neonates (5 males and 5 females)
 135 with birth weight adequate for gestational age (AGA) (mean
 136 gestational age 37.4). The clinical data of each patient were
 137 recorded in the hospital registers. Urine samples from the
 138 three groups were collected within 12 hours from birth (prior
 139 to feeding). Each urine sample (2–3 ml) was collected from
 140 the patients using a noninvasive method with a ball of cotton,
 141 then aspirated with a syringe and transferred to a sterile 15 ml
 142 Falcon tube. The tubes were then stored at -80°C until the
 143 time of the analysis using the GC-MS technique. An aliquot of
 144 100 μL from each sample formed a urine pooled sample to be
 145 analysed with the others as quality control sample.

147 Sample preparation

148 One-hundred fifty microliters of urine were transferred in
 149 glass vials (2 mL) with PTFE-lined screw caps and evaporated
 150 to dryness overnight in an Eppendorf vacuum centrifuge.
 151 30 μL of a 0.24 M solution of methoxylamine hydrochloride
 152 in pyridine was added to each vial, samples were vortex
 153 mixed and left to react for 17 h at room temperature. Then
 154 30 μL of MSTFA (N-Methyl-N-trimethylsilyl trifluoroaceta-
 155 mide) were added and left to react for 1 h at room
 156 temperature. The derivatized samples were diluted with
 157 hexane (300 μL) just before GC-MS analysis. The GC-MS
 158 analysis was performed on an Agilent 5975C interfaced to the
 159 GC 7820 equipped with a DB-5ms column (J & W), injector
 160 temperature at 230°C , detector temperature at 280°C , helium
 161 carrier gas flow rate of 1 ml/min. The GC oven temperature
 162 program was 90°C initial temperature with 1 min hold time
 163 and ramping at $10^{\circ}\text{C}/\text{min}$ to a final temperature of 270°C
 164 with 7 min hold time. 1 μL of the derivatized sample was
 165 injected in split (1:20) mode. After a solvent delay of
 166 3 minutes, mass spectra were acquired in full scan mode using
 167 2.28 scans/s with a mass range of 50–700 Amu.

170 Sample analysis

171 The chromatogram of the pooled sample was used to build a
 172 dedicated library of urinary metabolites: some chromato-
 173 graphic peaks were identified through comparison of reten-
 174 tion times and mass spectra with those obtained from
 175 authentic samples. Other metabolites were identified using
 176 the National Institute of Standards and Technology (NIST08)
 177 mass spectral database. In this way, 120 target compounds
 178 were identified, thus generating a custom library which was
 179 used for later automated analysis of samples by AMDIS

(Automated Mass Spectrometry Deconvolution and 181
 Identification System, <http://chemdata.nist.gov/mass-spc/> 182
 amd/s) software. 183

184 Mathematical model

185 Partial least squares discriminant analysis (PLS-DA) [5] is a
 186 multivariate classification model, which is similar to principal
 187 components analysis (PCA) [5], but unlike PCA maximizes
 188 the covariance in independent variables (metabolites) and a
 189 dependent variable (class labels, e.g. IUGR + LGA, AGA). To
 190 capture the maximum variance between clinically defined
 191 groups in the first dimension of the PLS-DA model, first
 192 latent variable (LV), all information orthogonal to group
 193 discrimination needs to be removed from the model.
 194 Unfortunately, the plane of separation between class scores
 195 in a preliminary PLS-DA model spanned two or more LVs
 196 (materials not shown). To simplify model interpretation of
 197 which variables had the greatest contribution to the discrim-
 198 ination between clinical classes [6–8], we implemented
 199 orthogonal signal correction-PLS (OSC-PLS) using the
 200 SIMCAP + 12 Umetrics software [5]. OSC-PLS discriminant
 201 analysis (OSC-PLS-DA) was used to maximize the captured
 202 variance between samples in the first dimension of the model
 203 (LV 1). We generated an OSC-PLS model based on our data
 204 and then used the resulting OSC-corrected data as input to
 205 generate an OSC-PLS-DA model. Variable loadings for the
 206 first LV were compared between PLS-DA and OSC-PLS-DA
 207 models. For most variables the magnitude of the model
 208 loading did not change greatly, but there were some param-
 209 eters whose sign for the loading changed; we needed to make
 210 sure that the sign of the variable loading accurately reflected
 211 each parameter's relative change between classes. In this way
 212 we specifically focused on how OSC affects the model's
 213 perception of the importance or weights of the variables
 214 resulting in significant differences in weights (delta weights)
 215 between a pure PLS-DA and an OSC-PLS-DA model. The
 216 primary step in this application of OSC filtering to a PLS-DA
 217 model is the building of the appropriate Y discrete-values
 218 function; the metabolic hypothesis may be tested with the
 219 function:
 220

$$y = 0 \quad \forall \text{ samples} \in \text{AGA}$$

$$y = 1 \quad \forall \text{ samples} \in \text{IUGR-LGA}$$

221 The Y column is added to the X matrix of the metabolite
 222 concentration and can be used to remove the orthogonal
 223 components in the X variance matrix. 224

225 Biomarker validation

226 Receiver Operating Characteristic (ROC) curves are generally
 227 considered the method of choice for evaluating the perform-
 228 ance of potential biomarkers. Some authors have developed a
 229 web-based tool designed to assist researchers in performing
 230 common ROC-based analyses on metabolomic data also using
 231 a multivariate approach [9]. The module provides a well-
 232 established approach based on the Partial Least Squares –
 233 Discriminant Analysis (PLS-DA) for classification and feature
 234 selection. Monte Carlo cross validation (MCCV) with mul-
 235 tiple iterations was employed to compute ROC curves and
 236
 237
 238
 239
 240

241 calculate confidence intervals of the AUCs. The purpose of
242 this module is to create and identify robust predictive models
243 using multiple biomarkers. The authors integrated feature
244 selection and classification procedures for the PLS-DA
245 algorithm. The procedures were repeated several times to
246 identify the best model as well as the most stable features.
247 The input for ROCET web tools is the data table containing
248 absolute or relative abundance values of compound concen-
249 trations. The file should be a data table with samples in rows
250 and features (metabolites) in columns; the phenotype labels
251 must follow immediately after the sample IDs. We uploaded
252 the OSC-X matrix filtered by means of the Y 2-values
253 classification function (classes for AGA versus IUGR-LGA).
254 Data were logarithmically transformed and Pareto scaled and
255 then the ROC analysis with the PLS-DA algorithm was
256 performed. The parameter for classifier performances, the
257 area under the ROC curve, was unitary due to the OSC
258 filtration action. A validation of the OSC-correction approach
259 was conducted in R [10] using the R package DeviumWeb
260 (<https://github.com/dgrapov/DeviumWeb>). DeviumWeb was
261 used to generate an OSC-PLS-DA model according to
262 previously published methods [11]. The sample scores and
263 variable importance rank were in close agreement between
264 the two approaches.

266 Results

268 Our GC-MS analysis of the urine samples showed significant
269 differences among AGA, LGA, and IUGR groups. A com-
270 parison between the chromatograms of urine samples collected
271 from AGAs, LGAs and IUGRs are shown in Figure 1.

272 As can be noted, quantitative and qualitative differences
273 are present among the groups. Subsequently, to elucidate the
274 association between the most important variables, a multi-
275 variate statistical approach was performed. The spectra of the
276 urine samples were aligned and the values of the relative
277 concentrations were placed in a numerical matrix with a size
278 of 33×111 . An explorative PCA model was built for all three
279 groups together and then for each group of subjects
280 (PCA class). Furthermore, to explore an innovative metabolic
281 hypothesis we later considered performing the analysis within
282 two groups: (1) LGA + IUGR, (2) AGA. The comparison
283 between these groups aimed to explore the common dysfunc-
284 tional pathways of LGA + IUGR, if they were present.
285 However, with an unsupervised approach the separation
286 among the three groups was not clear (data not shown). For
287 this reason, a method to extract the part of the covariant
288 metabolome using these two groups LGA + IUGR and AGA
289 was adopted. A new function with discrete arbitrary values
290 was created and the samples belonging to the LGA + IUGR
291 class had 1 value whilst the AGA class 0. The binary Y
292 variable created was subsequently used as the single Y
293 function for the OSC filter application to remove the non-
294 covariant part within the metabolic change of interest. After
295 OSC transformation of data, a PLS-DA model was built and a
296 clear separation between the groups (Figure 2) was found with
297 this OSC-PLS-DA model. The OSC-PLS-DA model gener-
298 ated had a high goodness of fit and predictability as
299 indicated by an R2Y value of 0.979 and a Q2 value of
300 0.903 respectively with a CV-ANOVA p value of 1.8×10^{-9} .

The analysis of the corresponding loading plot revealed 301
variables of importance for the clustering, thus allowing 302
identification of metabolites responsible for the variance 303
observed. The most important variable that significantly 304
contributed to the separation between the LGA + IUGR/AGA 305
groups was myo-inositol which was higher in the 306
LGA + IUGR group compared to AGA group. In addition, 307
the metabolites: urea, glycerol, glucose, citric acid and uric 308
acid were also important for clinical class discrimination. 309
A multivariate analysis of the OSC data was also performed 310
by means of the web tool MetaboAnalyst [9] with the 311
ROCET module used to calculate the ROC curves for 312
evaluation of the model classification power in terms of 313
sensibility and sensitivity (www.metaboanalyst.ca). The ROC 314
curve for myo-inositol showed an area under the curve almost 315
equal to 1 [Figure 3 left]. The following Figure 3 (right) 316
shows the box plot of the OSC-transformed concentrations of 317
myo-inositol OSC. 318

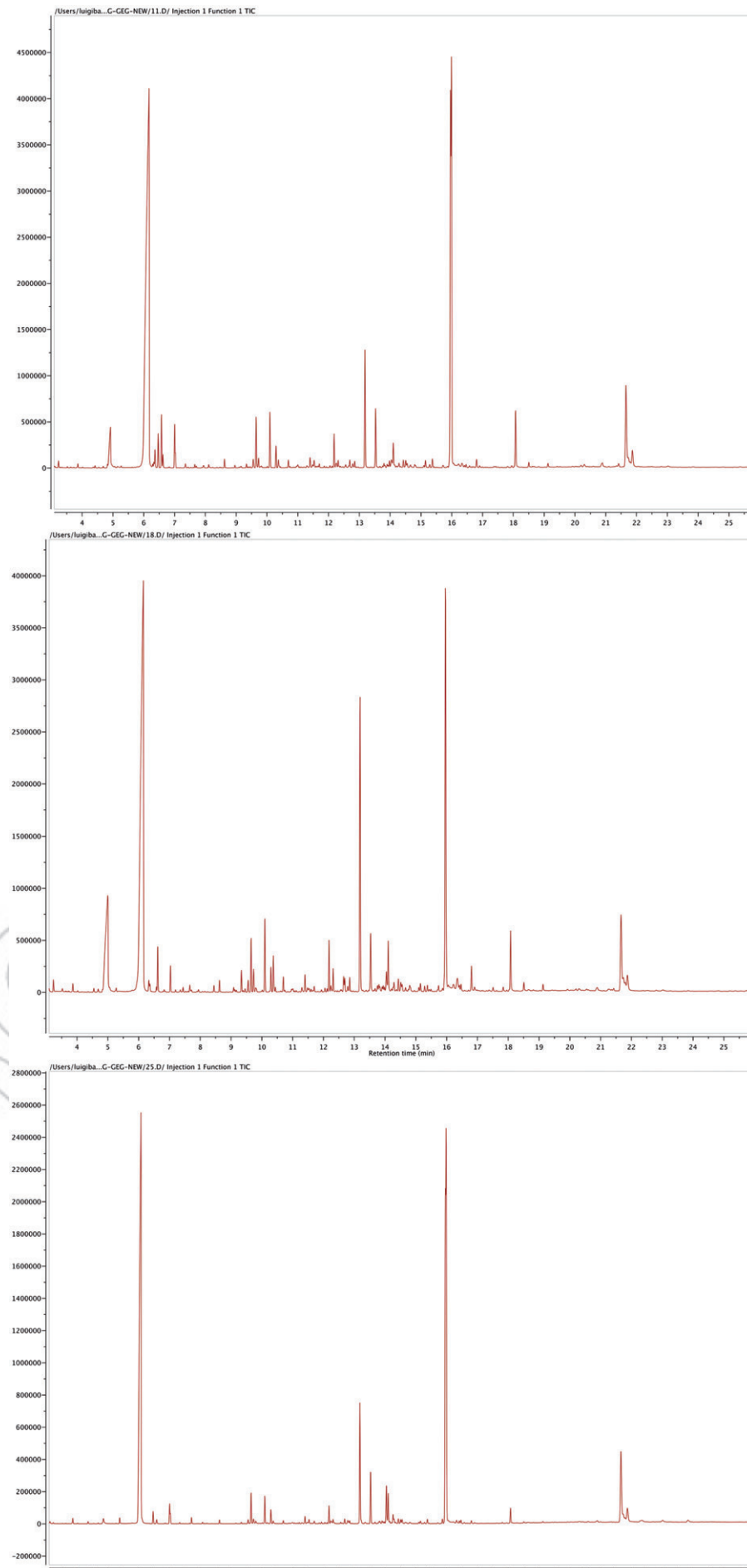
Data were processed also with the R software reproducing 319
results found with the SIMCAP12 (Figure 4). 320

322 Discussion

To date, little is known about the overall metabolic state of 324
IUGR and LGA neonates. In clinical practice, only a limited 325
number of metabolites are normally measured in neonates' 326
biological liquids by means of conventional analytical 327
methods. In recent years, metabolomics has assumed an 328
important clinical role since it is capable of making a 329
simultaneous qualitative and quantitative assessment of 330
a consistent number of metabolites in biological fluids so 331
as to supply a description of the present biochemical status of 332
an organism. Some studies in the literature correlate the 333
behavior of single substances such as inositol with intrauter- 334
ine growth retardation and suggest their possible role as 335
markers in such a pathology [12–14]. Inositol is a carbocyclic 336
polyol (the most important form in nature is myo-inositol) 337
which plays a fundamental role as the structural base of the 338
second messengers in eukaryotic cells, including the inositol 339
phosphates such as phosphatidylinositol and phosphatidyli- 340
nositol phosphate (PIP) [15]. It is an important metabolite for 341
different cell functions, among which cell growth and 342
survival, the development and functioning of peripheral 343
nerves, osteogenesis and reproduction. Many are the hor- 344
mones and neurotransmitters that trigger the production of 345
inositol following interaction with their receptors: classic 346
examples include insulin, serotonin, noradrenalin, histamine 347
and angiotensin. Certain organs such as the brain, the liver 348
and the pancreas have inositol concentrations up to 28 times 349
higher than those found in plasma; this emphasizes the 350
importance of this metabolite at the tissue and cellular levels. 351
In this study, the application of metabolomics made it 352
possible to identify molecules responsible for the differences 353
between the diverse metabolic profiles, among which myo- 354
inositol, whose urine content increased in IUGR and LGA 355
neonates compared to controls. Different inositol isomers 356
were found to possess insulin-mimetic properties and were 357
efficient in reducing post-prandial glucose levels in the blood. 358
Anomalies in the inositol metabolism were also associated 359
with insulin resistance and long-term microvascular 360

COLOR
Online /
B&W in
Print

Figure 1. GC/MS chromatograms of urine samples from LGA (top), AGA (middle), and IUGR (bottom) subjects.



361
362
363
364
365
366
367
368
369
370
371
372
373
374
375
376
377
378
379
380
381
382
383
384
385
386
387
388
389
390
391
392
393
394
395
396
397
398
399
400
401
402
403
404
405
406
407
408
409
410
411
412
413
414
415
416
417
418
419
420

421
422
423
424
425
426
427
428
429
430
431
432
433
434
435
436
437
438
439
440
441
442
443
444
445
446
447
448
449
450
451
452
453
454
455
456
457
458
459
460
461
462
463
464
465
466
467
468
469
470
471
472
473
474
475
476
477
478
479
480

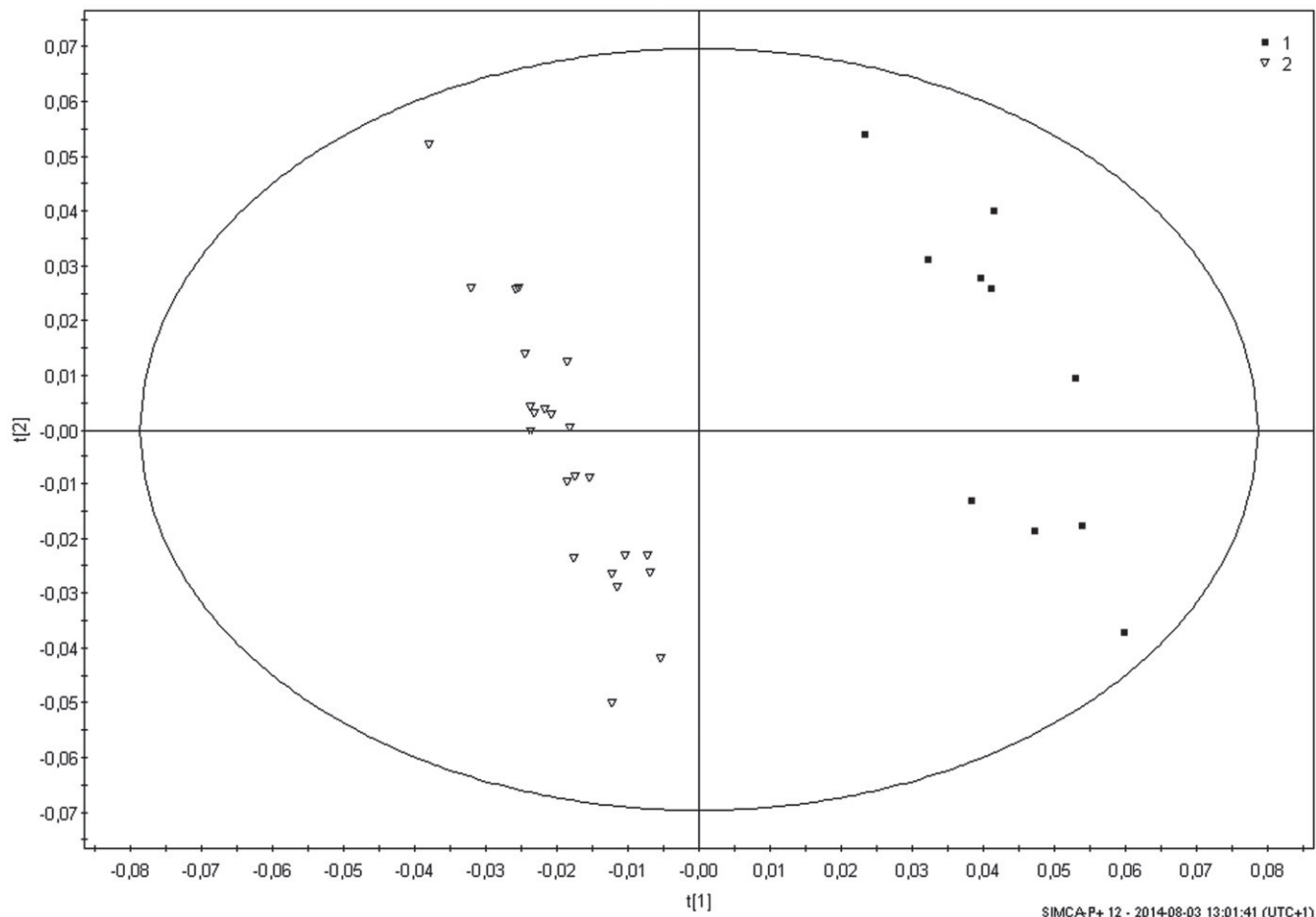
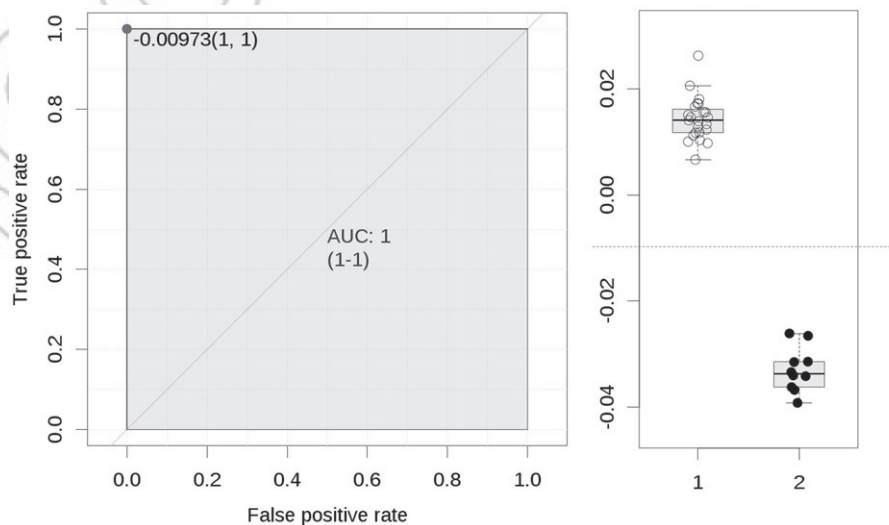


Figure 2. Score Plot of the OSC-PLS-DA model: 1 = black box AGA samples; 2 = Open Diamond LGA + IUGR samples.

Figure 3. Left: ROC curve for the Inositol OSC feature as biomarker; right: boxplot for the OSC-concentration values for the two classes 1 = AGA and 2 LGA + IUGR.



481
482
483
484
485
486
487
488
489
490
491
492
493
494
495
496
497
498
499
500
501
502
503
504
505
506
507
508
509
510
511
512
513
514
515
516
517
518
519
520
521
522
523
524
525
526
527
528
529
530
531
532
533
534 complications of diabetes, thus stressing a role of inositol or
535 its derivatives in the glucose metabolism [16]. In human
536 subjects with type 2 diabetes and experimental models (rhesus
537 monkeys, rats) there is an intracellular depletion of myo-
538 inositol with an increase in its secretion and at the same time a
539 decrease in the amount of D-chiro-inositol in the urine [17].
540 This kind of urinary excretion leads to a decrease in the

541
542
543
544
545
546
547
548
549
550
551
552
553
554
555
556
557
558
559
560
561
562
563
564
565
566
567
568
569
570
571
572
573
574
575
576
577
578
579
580
581
582
583
584
585
586
587
588
589
590
591
592
593
594 urinary [D-chiro-inositol]/[myo-inositol] ratio. The same
595 anomalous inositol behavior is to be seen in insulin-sensitive
596 tissues (liver, muscle, fat and kidneys) of human and animal
597 diabetic subjects [18]. Some researchers have found a
598 nonlinear, U-shaped association between birth weight and
599 type 2 diabetes which leads to an increased risk both for
600 neonates with high birth weight and those with low birth

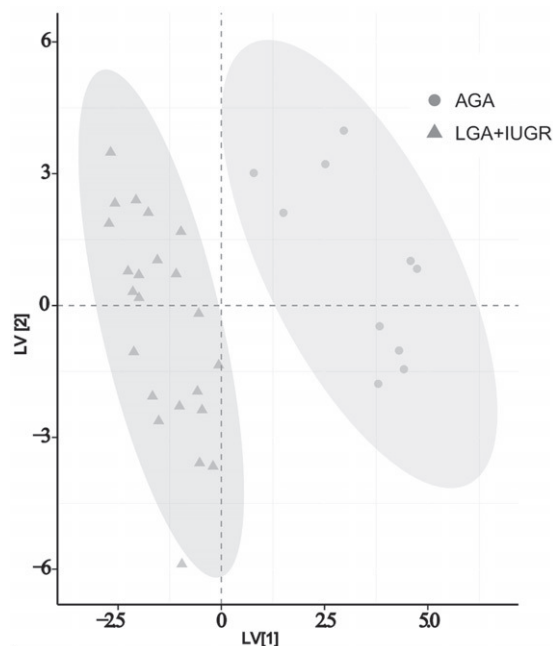


Figure 4. OSC-PLS-DA model calculated in R [10], which reproduced the previous results.

weight for their gestational ages [19]. This confirms what has been observed in cardiovascular [20] and kidney [21] pathologies. All this may explain the altered metabolic pattern found in IUGR and LGA neonates compared to controls and especially the increase in urinary myo-inositol that accumulates in the two pathologies. In this work, patients' urine samples were collected within 12 hours from birth when they had not yet been fed. The contribution of nutritive substances to the fetus is a key factor in the regulation of fetal growth. Many studies in the literature argue that environmental factors acting on the fetus (such as the kind of nutrition) may influence its prenatal development, thus determining structural and functional alterations that appear to be irreversible and continue in the course of postnatal life, leading to an increased risk of developing dysmetabolic diseases in adulthood. Several studies on animal models have confirmed that exposure to a hyper- and hypoglycemic environment in the uterus leads to a reduced glucose tolerance at birth which continues into adulthood, independently of subjects' genetic predisposition [22,23]. It is known that insulin plays a role in favoring lipid and protein synthesis as well as cell growth and inositol is known to be one of its important secondary messengers [24]. Up to now, works have been published to suggest that the glucose mechanism altered during fetal development in IUGRs may be marked by the increase in extracellular myo-inositol and some of these studies employed metabolomics in analyzing patients' samples [25,26]. This is the first work described in the literature that analyzed by means of metabolomics the urine metabolic profiles in IUGR and LGA neonates, comparing them to controls for the purpose of defining the metabolic patterns associated with such pathologies. The urinary increase in inositol (likely related to the high plasmatic concentrations of inositol), often associated with glucose intolerance and insulin resistance in adults, may also be considered valid markers of an altered glucose metabolism

during fetal development both in IUGRs and LGAs. It is thus to be hoped that future progress in metabolomics will soon make it possible to arrive at a more effective personalized nutritional therapy for the prevention of chronic adult pathologies in these patients.

Declarations of interest

The authors report no declarations of interest. The authors alone are responsible for the content and writing of the paper. One of the authors, Dmitry Grapov, is supported by a NIH Grant: NIH 1 U24 DK097154.

References

- Nicholson JK, Connelly J, Lindon JC, Holmes E. Metabonomics: a platform for studying 4 drug toxicity and gene function. *Nat Rev Drug Discov* 2002;1:153–61.
- Dessi A, Fanos V. Pediatric obesity: could metabolomics be a useful tool? *J Pediatr Neonatal Individualized Med* 2013;2:e020205.
- Dessi A, Puddu M, Ottonello G, Fanos V. Metabolomics and fetal-neonatal nutrition: between ‘not enough’ and ‘too much’. *Molecules* 2013;18:11724–32.
- Committee on Practice Bulletins – Gynecology, American College of Obstetricians and Gynecologists, Washington, DC 20090-6920, USA. Intrauterine growth restriction. Clinical management guidelines for obstetrician-gynecologists. American College of Obstetricians and Gynecologists. *Int J Gynaecol Obstet* 2001;72:85–96.
- Eriksson L, Johansson E, Kettaneh-Wold N, et al. Multi- and megavariable data analysis part II advanced applications and method extensions. Second edition ISBN-13: 978-91-973730-3-6.
- Wehrens R, Carvalho E, Masuero D, et al. High-throughput carotenoid profiling using multivariate curve resolution. *Anal Bioanal Chem* 2013;405:5075–86.
- Svensson O, Kourti T, MacGregor JF. An investigation of orthogonal signal correction algorithms and their characteristics. *J Chemometr* 2002;16:176–88.
- Smilowitz JT, Totten SM, Huang J, et al. Human milk secretory immunoglobulin-a and lactoferrin N-glycans are altered in women with gestational diabetes mellitus. *J Nutr* 2013;143:1906–12.
- Xia J, Broadhurst DI, Wilson M, Wishart DS. Translational biomarker discovery in clinical metabolomics: an introductory tutorial. *Metabolomics* 2013;9:280–99.
- R Core Team. R: A language and environment for statistical computing. R Foundation for Statistical Computing, Vienna, Austria. 2013. Available from: <http://www.R-project.org/>
- Wehrens R. Orthogonal signal correction and OPLS. In: Gentleman R, Hornik K, Parmigiani G, editors. *Chemometrics*. Berlin, Heidelberg: Springer-Verlag; 2011:240–3.
- Dessi A, Fanos V. Myo-inositol: a new marker of intrauterine growth restriction? *J Obstet Gynaecol* 2013;33:776–80.
- Kennington AS, Hill CR, Craig J, et al. Low urinary chiro-inositol excretion in non-insulin-dependent diabetes mellitus. *New Engl J Med* 1990;323:373–8.
- Ostlund Jr RE, McGill JB, Herskowitz I, et al. D-chiro-inositol metabolism in diabetes mellitus. *Proc Natl Acad Sci USA* 1993;90:9988–92.
- Downes CP, Macphee CH. Myo-inositol metabolites as cellular signals. *Eur J Biochem* 1990;193:1–18.
- Croze ML, Soulage CO. Potential role and therapeutic interests of myo-inositol in metabolic diseases. *Biochimie* 2013;95:1811–27.
- Sun TH, Heimark DB, Nguyen T, et al. Both myo-inositol to chiro-inositol epimerase activities and chiro-inositol to myo-inositol ratios are decreased in tissues of GK type 2 diabetic rats compared to Wistar controls. *Biochem Bioph Res Co* 2002;293:1092–8.
- Asplin I, Galasko G, Larner J. Chiro-inositol deficiency and insulin resistance: a comparison of the chiro-inositol- and the myo-inositol-containing insulin mediators isolated from urine, hemodialysate, and muscle of control and type II diabetic subjects. *Proc Natl Acad Sci USA* 1993;90:5924–8.

- 721 19. Harder T, Rodekamp E, Schellong K, et al. Birth weight and
722 subsequent risk of type 2 diabetes: a meta-analysis. *Am J Epidemiol*
723 2007;165:849–57. 781
- 724 20. Barker DJ, Osmond C. Infant mortality, childhood nutrition and
725 ischaemic heart disease in England and Wales. *Lancet* 1986;1:
726 1077–81. 782
- 727 21. Puddu M, Fanos V, Podda F, Zaffanello M. The kidney from
728 prenatal to adult life: perinatal programming and reduction of
729 number of nephrons during development. *Am J Nephrol* 2009;30:
730 162–70. 783
- 731 22. Holemans K, Aerts L, Van Assche FA. Lifetime consequences of
732 abnormal fetal pancreatic development. *J Physiol* 2003;547:11–20. 784
- 733 23. Fernandez-Twinn DS, Ozanne SE. Mechanisms by which poor early
734 growth programs type-2 diabetes, obesity and the metabolic
735 syndrome. *Physiol Behav* 2006;88:234–3. 785
- 736 24. Lam YY, Hatzinikolas G, Weir JM, et al. Insulin-
737 stimulated glucose uptake and pathways regulating energy
738 metabolism in skeletal muscle cells: The effects of subcutaneous
739 and visceral fat, and long-chain saturated, n-3 and n-6
740 polyunsaturated fatty acids. *Biochim Biophys Acta* 2011;1811:
741 468–575. 786
- 742 25. Nissen PM, Nebel C, Oksbjerg N, Bertram HC. Metabolomics
743 reveals relationship between plasma inositols and birth weight:
744 possible markers for fetal programming of type 2 diabetes.
745 *J Biomed Biotechnol* 2011. Available: [http://dx.doi.org/10.1155/
746 2011/378268](http://dx.doi.org/10.1155/2011/378268). 787
- 747 26. Dessì A, Atzori L, Noto A, et al. Metabolomics in newborns
748 with intrauterine growth retardation (IUGR): urine reveals
749 markers of metabolic syndrome. *J Matern-Fetal Neo M* 2011;24:
750 35–9. 788
- 751 789
- 752 790
- 753 791
- 754 792
- 755 793
- 756 794
- 757 795
- 758 796
- 759 797
- 760 798
- 761 799
- 762 800
- 763 801
- 764 802
- 765 803
- 766 804
- 767 805
- 768 806
- 769 807
- 770 808
- 771 809
- 772 810
- 773 811
- 774 812
- 775 813
- 776 814
- 777 815
- 778 816
- 779 817
- 780 818
- 819
- 820
- 821
- 822
- 823
- 824
- 825
- 826
- 827
- 828
- 829
- 830
- 831
- 832
- 833
- 834
- 835
- 836
- 837
- 838
- 839
- 840

PROOF ONLY

Q2